Sensors & Transducers, Vol. 187, Issue 4, April 2015, pp. 75-81

Sensors & Transducers

http://www.sensorsportal.com

Vibration-based Energy Harvesting Systems Characterization Using Automated Electronic Equipment

Ioannis KOSMADAKIS, Vasileios KONSTANTAKOS, Theodore LAOPOULOS, Stylianos SISKOS

Electronics Laboratory, Department of Physics, Aristotle University of Thessaloniki (AUTH), 56533, Greece

Tel.: +302310998138

E-mail: ikosm@physics.auth.gr

Received: 8 January 2015 /Accepted: 27 March 2015 /Published: 30 April 2015

Abstract: A measurement bench has been developed to fully automate the procedure for the characterization of a vibration-based energy scavenging system. The measurement system is capable of monitoring all important characteristics of a vibration harvesting system (input and output voltage, current, and other parameters, frequency and acceleration values, etc.). It is composed of a PC, typical digital measuring instruments (oscilloscope, waveform generator, etc.), certain sensors and actuators, along with a microcontroller based automation module. The automation of the procedure and the manipulation of the acquired data are performed by LabVIEW software. Typical measurements of a system consisting of a vibrating source, a vibration transducer and an active rectifier are presented. *Copyright © 2015 IFSA Publishing, S. L.*

Keywords: Automated measurement bench, Vibration monitoring, Energy harvesting, Piezoelectric cantilever, LabVIEW.

1. Introduction

A great effort to apply the ideas of renewable energy resources to the miniaturized world has been observed in research communities the past few years [1-7]. The conversion of low grade ambient environmental energy into useable electric energy is known as Energy Harvesting (EH) (aka Energy Scavenging).

The potential energy harvesting mechanisms can be categorized into four groups depending on the primary form of energy that is converted to electricity. These are:

a) Photovoltaic harvesting (light energy);
b) Vibrational harvesting (mechanical energy);
c) Thermal harvesting (thermal energy);
d) RF harvesting (electromagnetic energy) [7-14].

Although the most well known ambient source of energy is sunlight and photovoltaic energy conversion is considered to be a mature integrated circuit-compatible technology, it is limited to applications where sufficient sunlight is available.

In many applications where the use of solar is not practical (dark indoor areas), vibrations are used to extract the energy needed, since they are present in many environments (household appliances, industrial machines, automotives, buildings, structures etc.). There are three primary types of vibration to electric energy conversion mechanisms:

a) Electromagnetic;
b) Electrostatic;
c) Piezoelectric (PZT).

The main advances of PZT transduction, compared to the other two mechanisms, are its large

power density, its relatively higher output voltage and easy of application (no voltage source needed) [7, 14-17].

This work presents an automated measurement bench, which was designed and implemented to measure and characterize each part of a simple vibration-based piezoelectric energy harvesting system separately, as well as the whole system as one module [18]. The presented measurement bench allows systematic data acquisition and might be used for the measurement and the comparison of different harvesting systems, mechanisms and designs. It is capable of generating mechanical vibrations in a fully controlled range of 50-200 Hz, and then measuring all input and output parameters of the energy harvesting system (input and output currents and voltages, acceleration, frequency of vibrations).

2. Energy Harvesting System

A simple vibration-based piezoelectric energy scavenging system consists of

1) A vibrating source;

2) A PZT transducer;

3) An AC/DC converter (Fig. 1).

In the experimental EH system, the core of a simple medium size woofer (loudspeaker for low frequencies) is used as source of vibrations. The mechanical vibrations are then converted into electrical energy by a V25W PZT transducer from MIDE [19], connected in parallel configuration for increased output current.

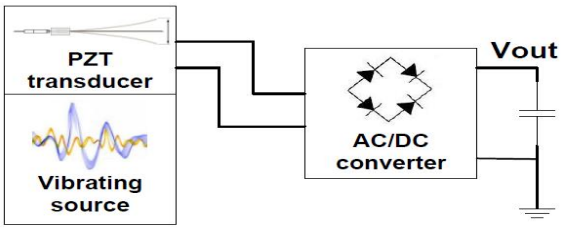

Fig. 1. Block diagram of a simple vibration-based piezoelectric energy harvesting system.

For the AC/DC conversion an integrated active rectifier [20-22], has been designed [23] in Cadence virtuoso 6.1.3 and fabricated using the AMS CMOS 0.35 um technology of Austria Microsystems. It is an output-powered, comparator-based converter, which is implemented by a MOSFET bridge rectifier in series with an "active" diode (a voltage comparator and a bulk-regulated p-MOS switch). This particular circuit was chosen to obtain low figures of power loss and maximum efficiency.

3. Automated Measurement Bench

The automated measurement bench is presented in Fig. 2. The excitation of the woofer is obtained by an HP33120A function waveform generator, while the resistive loads value is measured by an HP34401A digital multimeter. All the desired voltages are measured by a Yokogawa DL9140 digital oscilloscope. The atmega168 microcontroller (MCU) is used to implement the interface for

1) The MCP42100 digital potentiometer from Microchip (variable resistive load),

2) The 3-axis acceleration sensor ADXL345 from Analog Devices [24], which measures the acceleration values of the movements of the vibrating source.

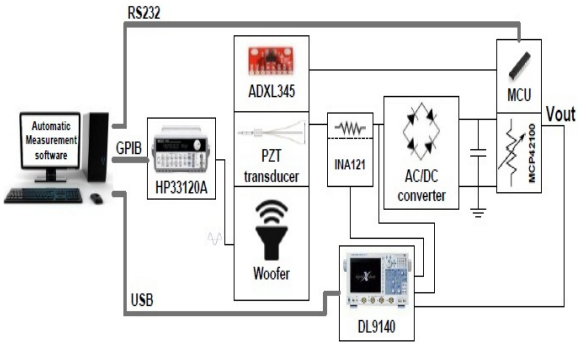

(a)

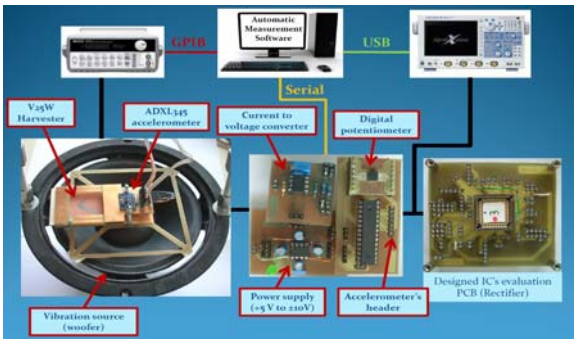

(b)

Fig. 2. Measurement bench for the characterization of the energy harvesting system: a) Block diagram and b) Setup.

SPI digital communication was selected between the MCU and its peripherals, so that maximum output data rate (3200 Hz) of the accelerometer is achieved.

A current to voltage converter was originated using the INA126 [25], which is a low power instrumentation amplifier from Texas Instruments, so that the small output current of the PZT transducer could be amplified and measured by the digital oscilloscope. The combination of the current to voltage converter and the digital oscilloscope could provide measurements of small currents and voltages in the time domain, which could be used for further analysis and description of the system under study.

A novel approach of systematic data acquisition in the time domain in order to measure all important characteristics of an experimental EH system is

proposed. Measured parameters include low level instantaneous current measurements, calculations of power, etc., using a fully automated setup instead of using just an rms multimeter as is quite common in recent literature [26-28].

The automation of the measurement bench and the control of all the peripheral equipment (measurement instruments, discrete electronics), is achieved using LabVIEW software from National Instruments, through GPIB, USB and RS232 interface. The same software (LabVIEW) performs the processing and storage of the acquired data.

4. Measurement Procedure

The measurement procedure is divided into four main steps. The individual measurement-characterization of each one of the three modules that compose the scavenging system, as previously described are:

1) Vibration source;
2) PZT transducer;
3) AC/DC converter on the one hand, and the measurement of the overall performance of the complete EH system on the other hand. Details for these four measurement steps are given in the following sections.

4.1. Source of Vibrations

Low level, low frequency (< 200 Hz) vibrations are examined, due to the wide range of applications in which the proposed system may be used [14].

Information, such as acceleration magnitude (α) and frequency (ω) of the vibrating source, is very useful since the potential output power for the vibration converter is proportional to α^2/ω [7].

The measurement bench for the vibrating source is shown in Fig. 3.

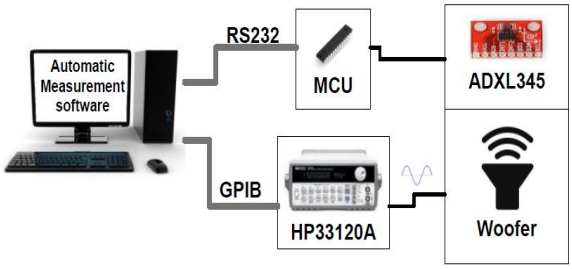

Fig. 3. Measurement bench for the characterization of the vibrating source.

The woofer is excited by a sinusoidal signal of varied amplitude and frequency. In each measurement the acceleration magnitude of all three axes (x, y, z) is acquired for a time duration of 5 seconds, having a full "picture" of the motion of the vibrating source. The maximum detected acceleration magnitude at z-axis, which is the main axis of movement (axis of harvester's displacement), is recorded. So a vibration spectrum of the woofer is available directly by the proposed system.

4.2. Piezoelectric Transducer

The previously described setup, with the harvester installed on the vibration source, could be used to reproduce a new vibration spectrum of the woofer and the harvester as one system/source.

The measurement bench for the PZT transducer is presented in Fig. 4.

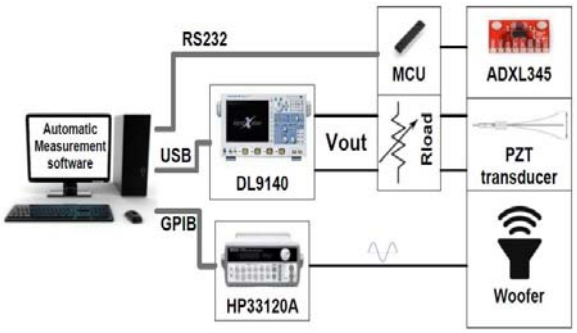

Fig. 4. Measurement bench for the characterization of the piezoelectric transducer.

This characterization procedure may be divided into two types of measurements:

a) Determination of the resonance frequency and
b) Determination of optimum resistive load.

The resonance frequency can be found by measuring the maximum detected open circuit voltage of the transducer all over the frequency range (50-200 Hz) of the excitation signal. Knowing the resonance frequency, the optimum load is determined by sweeping the resistive load and measuring the maximum output voltage ($P=V^2/R$). For a complete characterization of the transducer's behavior, the maximum output voltage (Vm_max), the output power (P) and the acceleration magnitude (α) could be measured for different amplitudes and frequencies of the excitation signal, as well as for different resistive loads.

4.3. Active Rectifier

The measurement bench for the designed active rectifier is shown in Fig. 5. The performance of the rectifier is measured by varying the output resistive load and by varying the frequency and the amplitude of an input sinusoidal signal. As mentioned above, the amplifier INA126 is configured as a current to voltage converter, in order to measure small input current. Using the current to voltage converter and the digital oscilloscope, the rectifier's behavior in the time domain can be studied. Input and output

currents and voltages can be measured and furthermore other characteristics, such as power, can be calculated. By making the appropriate measurements a full characterization of the performance of the rectifier can be achieved (power and voltage efficiency, ripple factor of the output signal etc.).

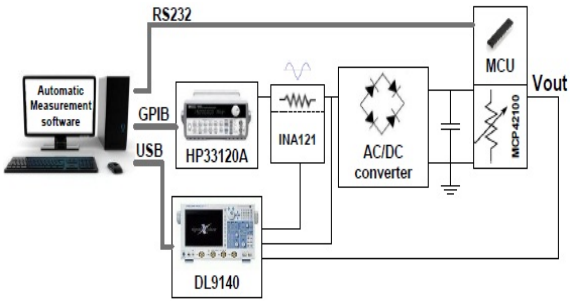

Fig. 5. Measurement Bench for the characterization of the designed active rectifier.

4.4. Vibration-Based Piezoelectric Energy Harvesting System

All previously described measurements can be applied to the measurement bench presented in Fig. 2, to fully characterize the complete experimental energy harvesting system.

The input and output voltage of the rectifier is directly measured by the digital oscilloscope, the output current of the PZT transducer is measured through the current to voltage converter (INA126) and the value of the resistive load is controlled by the software (through the MCU). Knowing these four values, the input and output power of the active rectifier can be calculated. Furthermore, the power efficiency of the EH system can be determined on the basis of this type of measurements. By sweeping

1) The frequency of the signal that excites the woofer,

2) The value of the resistive load, a full characterization of the system may be achieved.

5. Measurement Results

The measurement procedure presented above was followed to measure, study and fully characterize the experimental EH system described in Section II.

The maximum detected z-axis acceleration magnitude (z_acc_max) for varied amplitudes (Vampl) and frequencies of the excitation signal of the woofer, without the harvester installed, is showed in Fig. 6. It is clear that for the specific experimental system two areas of maximum performance are found near the vibration frequencies of 110 Hz and 145 Hz respectively. It is also shown that these values are not affected by the amplitude of the vibrations (four curves in Fig. 6).

Fig. 7 shows how the spectrum of the vibration source is affected by the harvester. A new peak of the maximum recorded z-axis acceleration magnitude is detected at the frequency of 80 Hz. In this point, it should be mentioned that for the protection of the transducer, mechanical breaks have been installed to keep the tip to tip displacement of the harvester in the maximum allowed limits. It is due to these mechanical limits that the measurement system detects a third peak in the area of 80 Hz (besides the other two mentioned above near the 110 Hz and 145 Hz). It is also due to these mechanical stop-points that the measured value of acceleration in the 80 Hz area is almost of double magnitude compared to the other two.

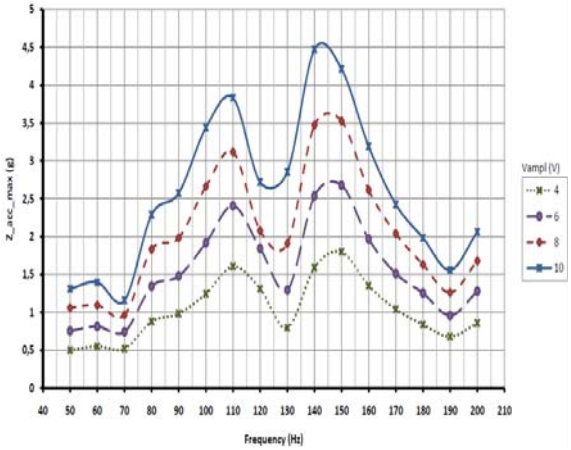

Fig. 6. Maximum detected z-axis acceleration magnitude of the vibration source for different amplitudes and frequencies of the excitation signal.

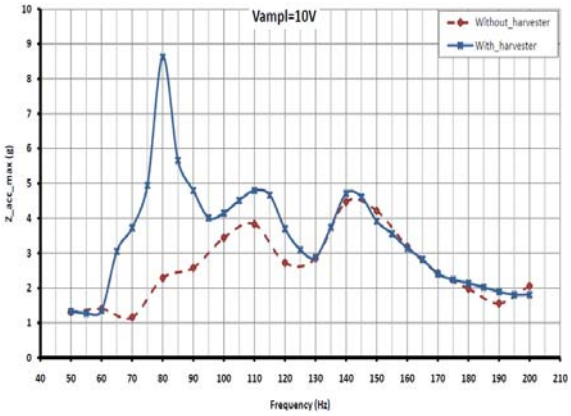

Fig. 7. Z-axis vibration spectrum of the source with and without the harvester, for the maximum available amplitude (10V) of the excitation signal.

Further results from the characterization of the PZT transducer are presented in Fig. 8 to Fig. 10. Fig. 8 illustrates the maximum detected open circuit voltage (V_op_crc_max) of the harvester for varied amplitudes (Vampl) and frequencies of the excitation signal. From this graph the resonance frequency of the whole experimental system of the transducer can

be determined (80 Hz).

Fig. 9 presents the frequency spectrum of the normalized open circuit voltage for an excitation signal of 10 V amplitude. Normalized open circuit voltage is calculated by dividing the maximum detected open circuit voltage with the maximum detected z-axis acceleration magnitude. As may be seen in Fig. 9 the experimental system is capable of providing a rather useful output signal all over a vibration frequency range of 65-140 Hz. Certain variations in the efficiency appear clearly within this range, but the main reason for these variations is probably caused by the specific mechanical structure used in the experimental measurements - not the harvesting system itself.

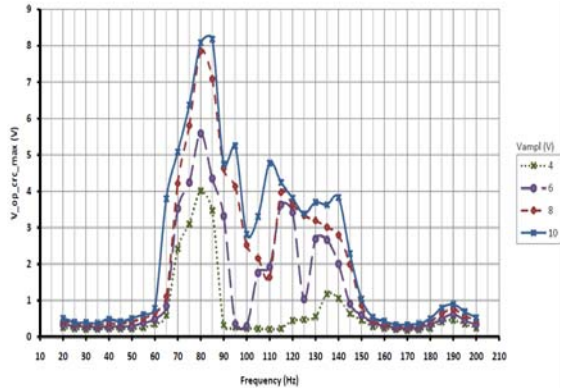

Fig. 8. Maximum open circuit voltage of the transducer for varied amplitudes and frequencies of the excitation signal.

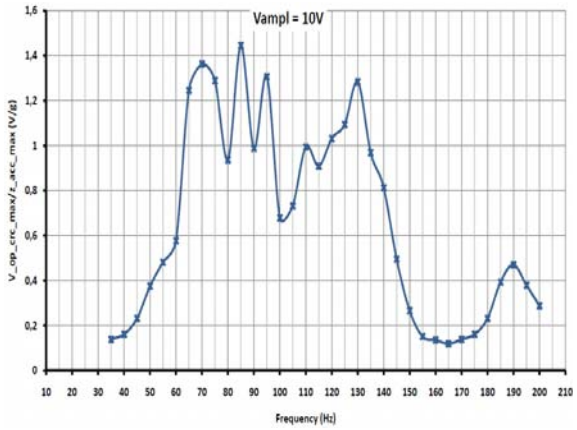

Fig. 9. Normalized open circuit voltage of the transducer for varied frequencies of the excitation signal (Vampl=10 V).

Fig. 10 depicts the maximum detected output voltage of the harvester for varied resistive loads, when the vibration source is driven by a sinusoidal signal of 10 V amplitude and 80 Hz frequency. It can be seen that for resistive loads of values lower than 10 kOhms, the output voltage decreases very fast. An important characteristic of the harvester used in the experimental measurements is shown clearly in this graph: the performance of the harvester is almost steady for a wide range of resistive loads (and thus for a range of output current values as well).

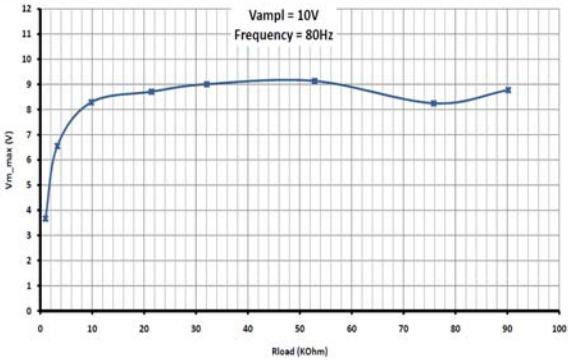

Fig. 10. Maximum output voltage of the harvester for varied resistive loads (excitation signal: 10 V, 80 Hz).

The power efficiency and the voltage conversion efficiency (100*Vout/Vin) of the designed rectifier, for different resistive loads and an input sinusoidal signal of varied amplitude (Vampl) and frequency of 100 Hz, are shown in Fig. 11 and Fig. 12 respectively.

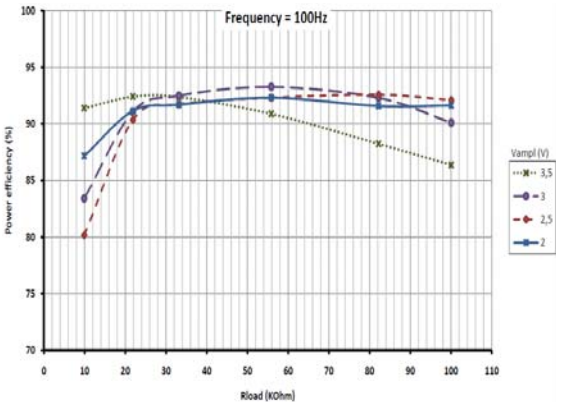

Fig. 11. Power efficiency of the designed active rectifier for an input signal of 100 Hz frequency and varied amplitudes.

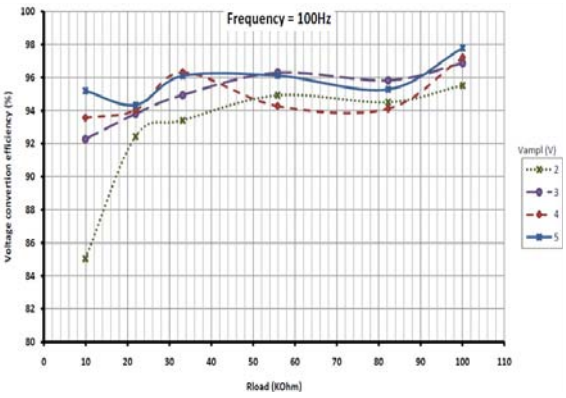

Fig. 12. Voltage conversion efficiency of the designed active rectifier for an input signal of 100 Hz frequency and varied amplitudes.

For the measurements of the whole EH system, the amplitude of the excitation signal was the maximum available (10 V). Fig. 13 presents the power efficiency of the experimental EH system for varied resistive loads and selected frequencies as they arise from diagram in Fig. 8. It should be noted that as it was expected, the power efficiency of the system decreases rapidly when the load becomes smaller than approximately 10 kOhms (optimum load of the harvester). System's response remains almost steady for a wide range of smaller loads (bigger resistance values). Yet, a different (and more useful) picture of the same phenomenon is shown in Fig. 14 which presents the output power of the EH system for different loads all over the frequency range of interest. The peak of the harvested power near the 80 Hz frequency where the maximum of acceleration was measured is again very clear. Other peaks of smaller magnitude in the areas of 95 Hz, 115 Hz, and near 140 Hz are also measured in accordance with the results presented in Fig. 9.

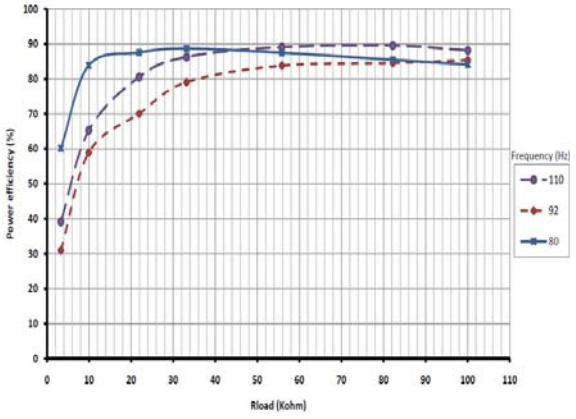

Fig. 13. Power efficiency of the EH system for varied resistive loads and selected frequencies.

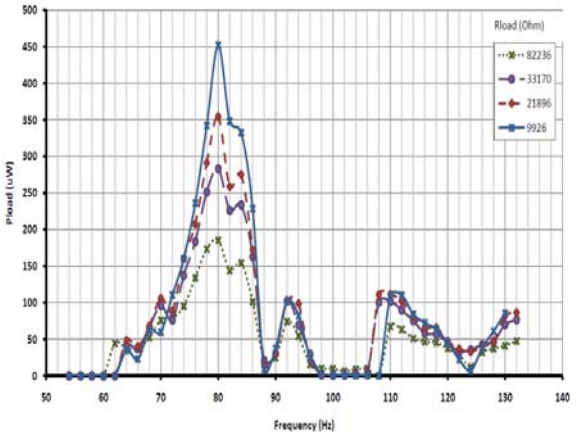

Fig. 14. Harvested power for varied frequencies and loads.

Finally, from the diagram in Fig. 15 it can be seen that at the frequency of 80 Hz and for a resistive load of approximately 10 kOhms, the maximum power of 452.48 μW is harvested. At this point of operation, a power efficiency of 83.9 % is calculated, illustrating thus clearly the overall system's performance. This value remains steady though, throughout the range of interest for the resistive loads indicating the efficient use of the specific harvesting system for a rather wide range of applications (regarding their power consumption).

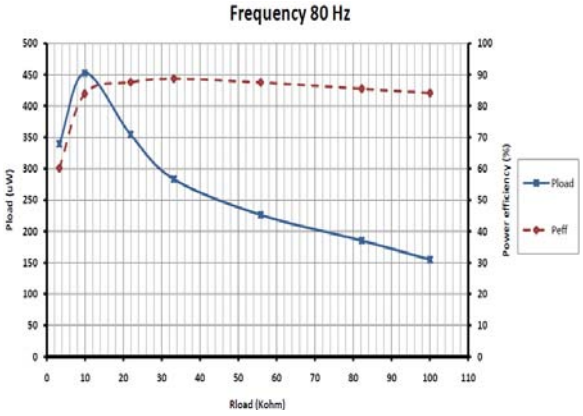

Fig. 15. Output power and power efficiency of the EH system for different resistive loads.

6. Conclusions

A novel configuration for an automated measurement bench for vibration-based energy harvesting systems is introduced. The measurement procedure for a complete characterization of the performance of an experimental Energy Harvesting system, either as a whole, or separately in the different sub-modules, is described. Typical results illustrating the measurement capabilities of the proposed automated measurements configuration are provided. Such a detailed measurement sequence is very useful for an effective characterization and comparison of various harvesting systems in different applications.

References

[1]. Y. K. Ramadass, A. P. Chandrakasan, An efficient piezoelectric energy harvesting interface circuit using a bias-flip rectifier and shared inductor, *IEEE Journal of Solid-State Circuit*, Vol. 45, Issue 1, 2010, pp. 189-204.

[2]. E. O. Torres, G. A. Rincon-Mora, A 0.7-μm BiCMOS electrostatic energy-harvesting system IC, *IEEE Journal of Solid-State Circuit*, Vol. 45, Issue 2, 2010, pp. 483-496.

[3]. E. E. Aktakka, R. L. Peterson, K. Najafi, A self-supplied inertial piezoelectric energy harvester with power-management IC, in *Proceedings of the IEEE International Solid-State Circuits Conference Digest of Technical Papers (ISSCC'11)*, San Francisco, CA, 20-24 February 2011, pp. 120-121.

[4]. A. Harb, Energy harvesting: State-of-the-art, *Renewable Energy*, Vol. 36, Issue 10, 2011, pp. 2641-2654.
[5]. D. Maurath, P. F. Becker, D. Spreemann, Y. Manoli, Efficient energy harvesting with electromagnetic energy transducers using active low-voltage rectification and maximum power point tracking, *IEEE Journal of Solid-State Circuit*, Vol. 47, Issue 6, 2012, pp. 1369-1380.
[6]. S. Tornincasa, M. Repetto, E. Bonisoli, F. Di Monaco, Energy harvester for vehicle tires: Nonlinear dynamics and experimental outcomes, *Journal of Intelligent Material Systems and Structures*, Vol. 23, Issue 1, 2012, pp. 3-13.
[7]. C. Ó Mathúna, T. O'Donnell, R. V. Martinez-Catala, J. Rohan, B. O'Flynn, Energy scavenging for long-term deployable wireless sensor networks, *Talanta*, Vol. 75, Issue 3, 2008, pp. 613-623.
[8]. J. Colomer-Farrarons, P. Miribel, A CMOS Self-Powered Front-End Architecture for Subcutaneous Event-Detector Devices, *Springer*, 2011.
[9]. T. O'Donnell, W. Wang, Power Management, Energy Conversion and Energy Scavenging for Smart Systems, in Kieran Delaney (Ed.), Ambient Intelligence with Microsystems, *Springer*, 2009, pp. 241-266.
[10]. K. A. Cook-Chennault, N. Thambi, A. M. Sastry, Powering MEMS portable devices — a review of non-regenerative and regenerative power supply systems with special emphasis on piezoelectric energy harvesting systems, *Smart Materials and Structures*, Vol. 17, Issue 4, 2008, 043001.
[11]. H. J. Visser, A. C. F. Reniers, J. A. C. Theeuwes, Ambient RF Energy Scavenging: GSM and WLAN Power Density Measurements, in *Proceedings of the Conference on 38th European Microwave Conference (EUMC'08)*, Amsterdam, Netherlands, 27-31 October 2008, pp. 721-724.
[12]. M. T. Penella-López, M. Gasulla-Forner, Powering Autonomous Sensors, *Springer*, 2011.
[13]. Y. Manoli, Th. Hehn, D. Hoffmann, M. Kuhl, N. Lotze, D. Maurath, Chr. Moranz, D. Rossbach, D. Spreemann, Chips 2020 - A Guide to the Future of Nanoelectronics, B. Hoefflinger (Ed.), *Springer*, 2012.
[14]. S. Roundy, P. K. Wright, J. Rabaey, A study of low level vibrations as a power source for wireless sensor nodes, *Computer Communications*, Vol. 26, Issue 11, 2003, pp. 1131-1144.
[15]. A. Erturk, D. J. Inman, Piezoelectric energy harvesting, *John Wiley & Sons*, 2011.
[16]. T. J. Kaźmierski, St. Beeby, Energy Harvesting Systems: Principles, Modeling and Applications, *Springer*, 2011.
[17]. N. Elvin, A. Erturk, Advances in Energy Harvesting Methods, *Springer*, 2013.
[18]. I. Kosmadakis, V. Konstantakos, Th. Laopoulos, St. Siskos, An Automated Measurement Bench for Vibration-based Energy Harvesting Systems, in *Proceedings of the 7th IEEE International Conference on Intelligent Data Acquisition and Advanced Computing Systems (IDAACS'13)*, Vol. 1, Berlin, Germany, 12-14 September 2013, pp. 15-20.
[19]. MIDE Web Portal (http://www.mide.com).
[20]. C. Peters, D. Spreemann, M. Ortmanns, Y. Manoli, A CMOS integrated voltage and power efficient AC/DC converter for energy harvesting applications, *Journal of Micromechanics and Microengineering*, *JMM*, Vol. 18, Issue 10, 2008, 104005.
[21]. C. Peters, M. Ortmanns, Y. Manoli, Fully CMOS integrated active rectifier without voltage drop, in *Proceedings of the 51st Midwest Symposium on Circuits and Systems (MWSCAS'08)*, Knoxville, TN, 10-13 August 2008, pp. 185-188.
[22]. Y. Rao, D. P. Arnold, Input-powered energy harvesting interface circuits with zero standby power, in *Proceedings of the 26th Annual IEEE Applied Power Electronics Conference and Exposition (APEC'11)*, Fort Worth, TX, 6-11 March 2011, pp. 1992-1999.
[23]. I. Kosmadakis, Th. Laopoulos, St. Siskos, Design of Energy Harvesting Electronics in AMS035, in *Proceedings of the Panhellenic Conference on Electronics and Telecommunications (PACET'12)*, Thessaloniki, Greece, 16-18 March 2012.
[24]. Analog Devices (http://www.analog.com).
[25]. Texas Instruments (http://www.ti.com).
[26]. A. Rahimi, Ö. Zorlu, A. Muhtaroglu, H. Külah, Fully self-powered electromagnetic energy harvesting system with highly efficient dual rail output, *IEEE Sensors Journal*, Vol. 12, Issue 6, 2012, pp. 2287-2298.
[27]. J. Lee Wardlaw, A. Ilker Karsılayan, Self-powered rectifier for energy harvesting applications, *IEEE Journal on Emerging and Selected Topics in Circuits and Systems*, Vol. 1, Issue 3, 2011, pp. 308-320.
[28]. R. Elfrink, T. M. Kamel, M. Goedbloed, S. Matova, D. Hohlfeld, Y. van Andel, R. van Schaijk, Vibration energy harvesting with aluminum nitride-based piezoelectric devices, *Journal of Micromechanics and Microengineering*, Vol. 19, Issue 9, 2009, 094005.